Aqueous Only Route toward Graphene from Graphite Oxide

Ken-Hsuan Liao, Anudha Mittal, Shameek Bose, Christopher Leighton, K. Andre Mkhoyan,* and Christopher W. Macosko*

Department of Chemical Engineering and Materials Science, University of Minnesota, Minneapolis, Minnesota 55455, United States

ABSTRACT We report a new, simple, hydrazine-free, high-yield method for producing single-layer graphene sheets. Graphene sheets were formed from graphite oxide by reduction with simple deionized water at 95 °C under atmospheric pressure. Over 65% of the sheets are single graphene layers; the average sheet diameter is 300 nm. We speculate that dehydration of graphene oxide is the main mechanism for oxygen reduction and transformation of C—C bonds from sp^3 to sp^2. The reduction appears to occur in large uniform interconnected oxygen-free patches so that despite the presence of residual oxygen the sp^2 carbon bonds formed on the sheets are sufficient to provide electronic properties comparable to reduced graphene sheets obtained using other methods.

KEYWORDS: graphene · graphene oxide · aqueous route · oxygen reduction · dehydration

Graphene has zero band gap and high carrier concentrations and mobilities and, as a result, exhibits remarkable electronic properties.[1,2] For reliable integration of graphene into practical electronic devices it is essential to have a simple, reproducible, and controllable technique to produce large-area graphene sheets on a large scale. Micromechanical cleaving,[3] exfoliation of individual graphene sheets *via* sonication in solvent,[4,5] and growth of graphene on SiC or nickel substrates[6−8] have been reported as possible techniques to produce graphene. However, reduction of graphene from exfoliated graphite oxide/graphene oxide (XGO) appears to be the most promising approach for large-scale production.[9−13]

XGO can be obtained with a range of O:C stoichiometries depending on the details of the particular synthesis. In XGO sheets the oxygen is bound to the carbon in the form of hydroxyl and epoxy functional groups[14,15] and some carbonyl.[16] Several reports suggest that XGO can be reduced to graphene either chemically by exposing XGO to hydrazine (as a hydrate, as anhydrous hydrazine, or as dimethylhydrazine vapor)[9,17−19] or by rapid heating to high temperature[11] or, alternatively, a combination of both.[10,13,16,19] Toxicity of hydrazine and the necessity of extreme temperatures, ~1000 °C for the thermal route, make it desirable to seek other reduction methods. Here we describe a new hydrazine-free and aqueous only route toward reduction of graphene from XGO at atmospheric pressure and moderate temperature. Other water-based reduction of graphene has been reported previously by Zhou *et al.*,[20] Chen *et al.*,[21] and Chen *et al.*[22]

RESULTS AND DISCUSSION

Large exfoliated individual graphene sheets (GS) were obtained following a three-step process: (i) transition from graphite into graphite oxide (GO), (ii) intercalation of GO with water to form XGO, and, finally, (iii) exfoliation with conversion of XGO into GS. In the first step GO was synthesized from graphite, with an average particle size of 30 μm, using a modified Hummer's method[23] (the details can be found in the Supporting Information, SI). Wide-angle X-ray diffraction (WXRD) measurements were performed on the original graphite and the obtained GO, Figure 1. Dry powders of graphite and GO were used here. The measurements confirm the expected shift in the main peak: the 2θ Bragg angle moved from 26.5°, corresponding to d_{0001}= 0.34 nm spacing between atomic planes in graphite, to 10.1° in GO, which corresponds to an interplane distance of d_{0001}= 0.94 nm.[24,25]

In the second step, GO particles were dispersed in DI water at a concentration of about 0.9 mg/mL (pH ≈ 3), then sonicated for about 1 h at room temperature[26] (at 40 kHz with power of 100 W). The WXRD measurement from XGO powder, which was filtered and dried in a vacuum oven at 45 °C for 24 h, presented in Figure 1, shows further position reduction and broadening of the Bragg peak to $2\theta = 8°$ (d = 1.12 nm). We speculate that the 0.22 nm increase in distance between exfoliated layers is due to water swelling

*Address correspondence to mkhoyan@umn.edu, macosko@umn.edu.

Received for review October 26, 2010 and accepted January 12, 2011.

Published online January 27, 2011
10.1021/nn1028967

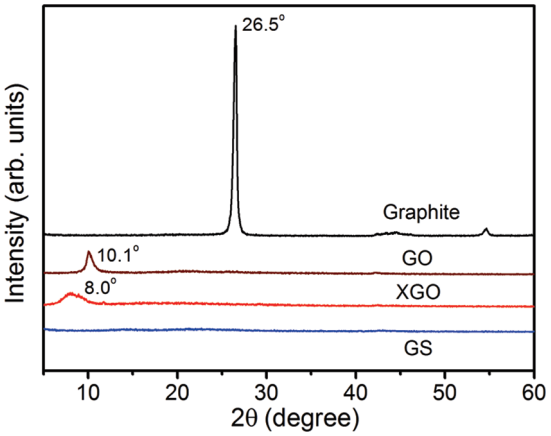

Figure 1. WXRD measurements from graphite, graphite oxide (GO), exfoliated graphite oxide (XGO), and graphene sheets (GS) obtained at different stages of graphite to graphene transition.

of GO during sonication. The increase in *d*-spacing is slightly less than the size of a water molecule, ~0.28 nm. XGO layers are not perfectly flat. A roughness of ~0.6 nm has been measured,[27] which may provide space to accommodate water molecules.

X-ray photoelectron spectroscopy (XPS) and elemental analysis (EA) were performed on these XGO sheets. Figure 2a shows that the C^{1s} spectrum is a superposition of two strong peaks at 286.2 and 284.4 eV that are fingerprints of C−O (including epoxy and hydroxyl groups) and C−C bonds.[16,28,29] Decomposition of the C^{1s} XPS spectrum into these main components indicates that the fractions of C−O and C−C bonds in XGO are 70% and 30%, respectively. Although some C═O and C(═O)−(OH) bonds (with corresponding peaks at 287.5 and 289.2 eV) are also expected to be present in XGO,[17] no visible amounts are detected in these samples. Analysis of the XPS measurements, including the intensities of the spectra of C and O K-edges, indicates that the oxygen to carbon ratio in XGO is close to O:C = 1:2. The same ratio is also found from the standard EA measurements (see SI). Since it is energetically favorable for oxygen to be bonded to two carbon atoms,[27] the XPS and EA measurements indicate that at this stage the XGO sheets are heavily oxidized, which is in good agreement with previous reports.[2,16,28]

To obtain GS from these XGO, the sample was heated in DI water at 95 °C for more than 70 h. XPS measurements performed on the final material show a significant drop in C−O relative to C−C bonds (see Figure 2b). Decomposition of the C^{1s} XPS spectrum obtained from GS into components indicates that the fractions of C−O and C−C bonds now are 31% and 69%, respectively. The ratio of oxygen to carbon is reduced to about O:C = 1:6, a value confirmed by EA (see SI). Stankovich et al.[9] reported that the ratio O:C of hydrazine-reduced XGO can be as low as 1:10.3. However, the reduction process is accompanied by nitrogen incorporation with ratio N:C = 1:16.1, which results in (O+N):C = 1:6.

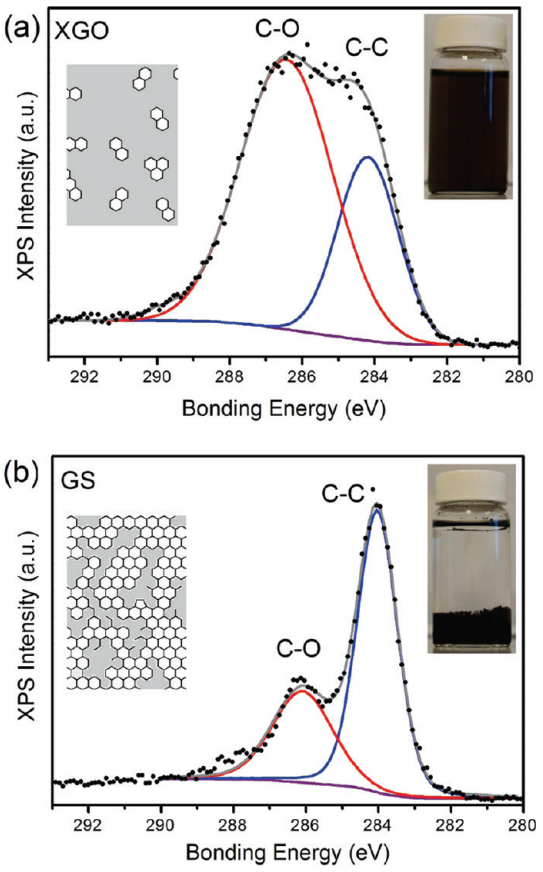

Figure 2. C^{1s} XPS spectra and a simple molecular model describing the structures (inset on left-hand side) of (a) XGO and (b) GS showing reduction of C−O bonds from XGO to GS. The insets in upper-right corners are suspensions of XGO and GS in DI water (pH ≈ 3), correspondingly.

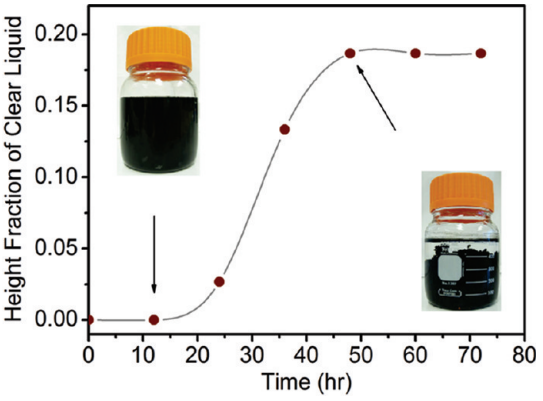

Figure 3. Transformation of XGO to GS in DI water (pH ≈ 3) at 95 °C as a function of time. Initial XGO suspension is shown in the left vial. After 48 h black and "fluffy" precipitates with nonpolar C−C bonds are observed (right vial).

Figure 3 shows that at 95 °C the XGO to GS transformation is completed within 48 h. The appearance of black "fluffy" precipitates at the end of transformation is indicative of a dramatic increase of nonpolar C−C bonds and thus reduction. Using the same procedure at 80 °C did not produce the XGO to GS transformation even after 5 days. At 120 °C (see SI) GS with the same characteristics as at 95 °C was obtained after 12 h.

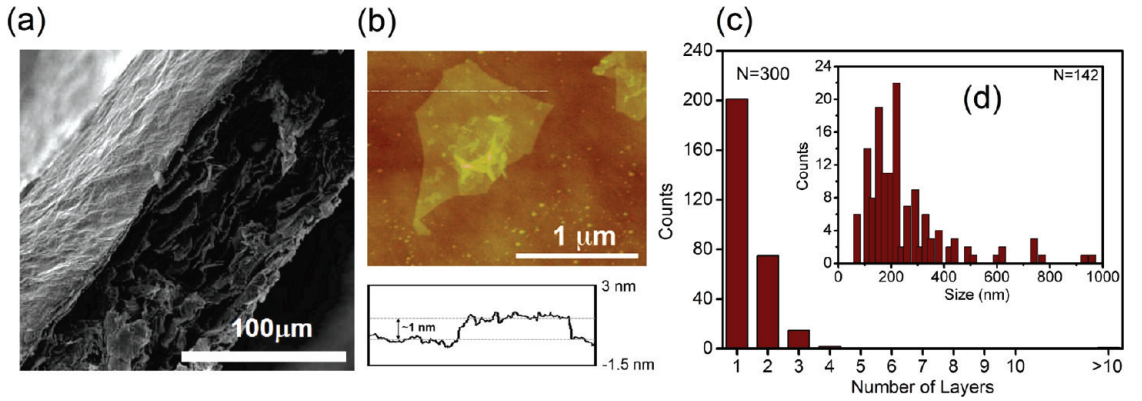

Figure 4. GS reduced from XGO after 48 h at 95 °C in DI water (pH = 3). (a) SEM image of GS film of many GS sheets. (b) AFM image of a single GS sheet (top) with thickness profile across the flake (bottom). (c) Histogram of number of layers per particle and (d) sheet sizes of GS.

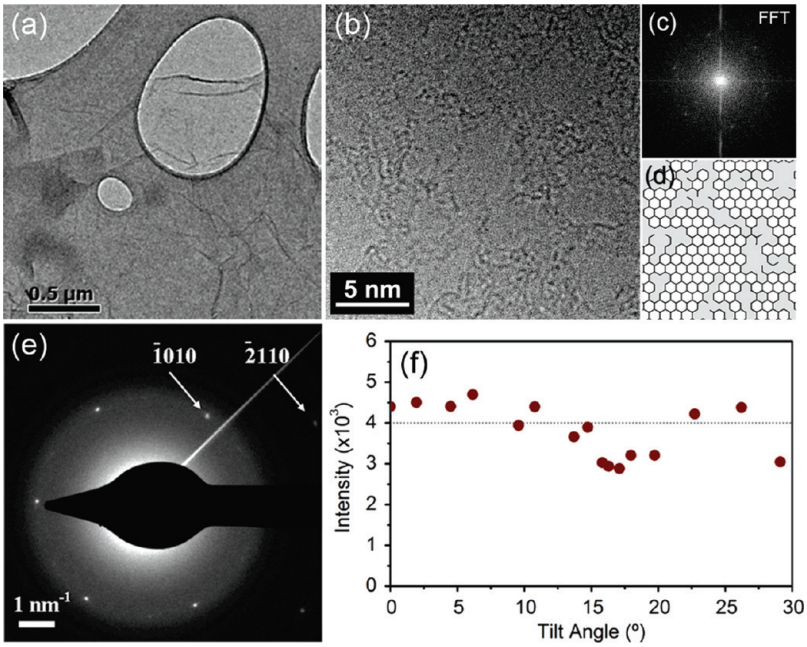

Figure 5. (a) Low-magnification TEM image of GS suspended over holey-carbon film showing typical wrinkles occurring in most sheets. (b) High-magnification TEM image of GS showing amorphous and crystalline regions. (c) FFT from crystalline regions of the image in (b) showing hexagonal symmetry. (d) Schemetic of (b) where hexagons represent crystalline regions and gray represents amorphous. (e) Electron diffraction pattern from GS. (f) Change in intensity of $\bar{1}010$ spot as the GS is tilted relative to incident beam.

Despite that a considerable amount of oxygen is still present in the GS, the sheets have very low electrical resistance. The ratio of the resistance measured at room temperature from similarly prepared thin films of GS as XGO (both with thickness of about 40 μm) was found to be $R_{GS}/R_{XGO} \approx 4 \times 10^{-5}$ (see SI). A SEM image of a typical GS film is presented in Figure 4a. Such 5 orders of magnitude reduction in resistance going from XGO to GS was also reported by Stankovich *et al.*,[9] Eda and Chhowalla,[10] and Mattevi *et al.*[16] after hydrazine or heat treatment. The resistances of XGO and GS are highly sensitive to the fractions of the sp^2 and sp^3 bonds of carbon atoms in the sheets and concentration of oxygen atoms, which act as scattering centers. While reduction of oxygen in XGO is essential for minimizing the density of scattering centers, its effects on sp^3 to sp^2 transitions of carbon bonds are not clear. Our measurements indicate that, despite the relatively large fraction of oxygen still remaining in the GS, the oxygen reduction method described here provides sheets that contain large interconnected patches of oxygen-free graphene with sp^2 bonds.

Thicknesses of 300 individual GS were measured using atomic force microscopy (AFM) (Figure 4 and SI). The thickness of individual GS is about 1 nm, which is smaller than 1.6 nm, the reported thickness of XGO,[28] consistent with thickness measurements of graphene.[31,32]

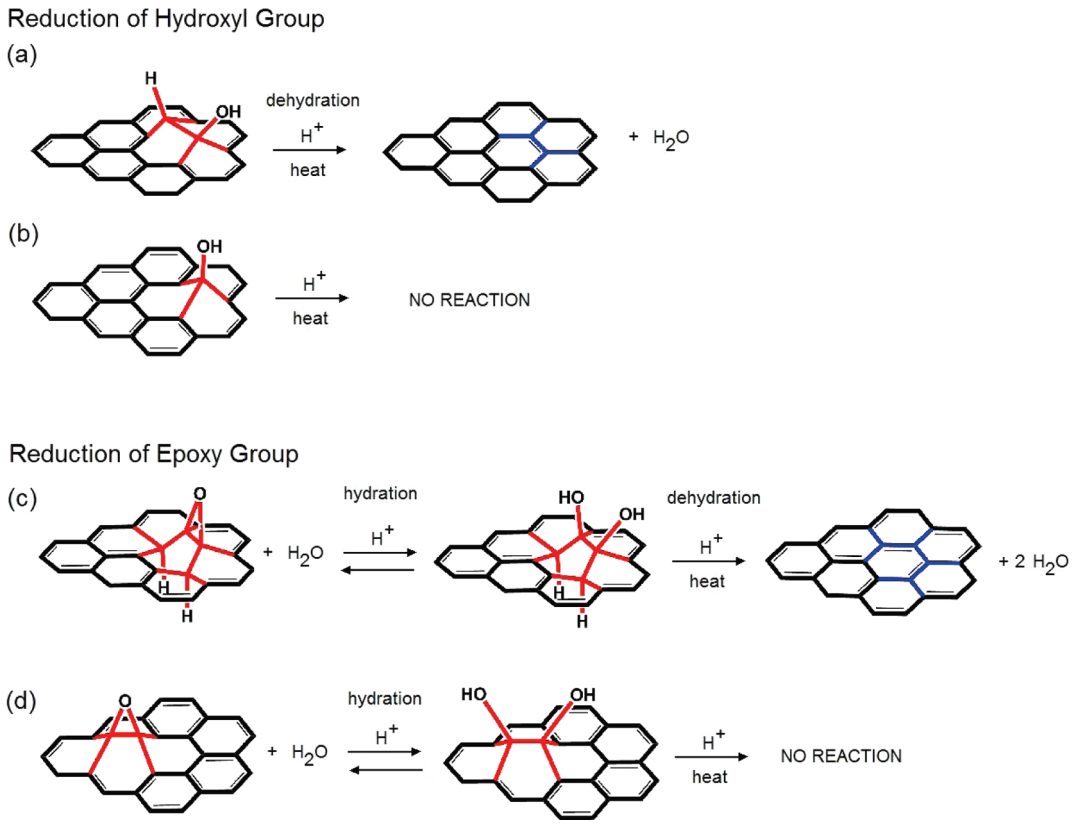

Figure 6. Shematic diagrams for reduction of hydroxyl and epoxy groups for XGO to GS transformation.

The statistical analysis of AFM measurements indicates that approximately 65% of the sheets are single layers (with thicknesses ranging from 0.6 to 1.2 nm), 27% are double layered (1.2−2.4 nm), and the remaining 8% are multilayered (>2.4 nm; Figure 4c). The average diameter of GS is ~300 nm (see Figure 4d).

Transmission electron microscopy (TEM) was used to further analyze oxygen-reduced GS. Figure 5a shows a low-magnification image of a typical GS suspended over the holey-carbon film covering a standard TEM copper grid. All expected characteristics of the single sheet, including numerous wrinkles, can be seen. Detailed examination of high-resolution images of individual sheets (see Figure 5b) suggests that the sheet consists of two regions: (i) large uniform regions of minimum contrast variation and hexagonal symmetry, which can be seen in the fast Fourier transform (FFT) pattern shown in Figure 5c, and, (ii) amorphous-like regions in between with strong contrast variation. The uniform areas in the sheets are characteristic of oxygen-free regions,[33] and the fact that they are connected is consistent with resistance measurements. These regions make up ~50% of the area in the high-resolution image. If we assume that the area appearing amorphous is due to oxidation and that the O:C ratio in these areas is 1:2, then based on the area ratios the total sheets should have an O:C ratio of 1:6. This is in agreement with our XPS and EA results.

To confirm that the layers studied here are indeed single layers of GS, we analyzed the change in intensity of the $\bar{1}010$ diffraction spot as the sample was tilted with respect to the incident beam over a range of 30 degrees. For an infinitely thin sample, the intensity should remain constant as the sample is tilted. A single-atomic-layer-thin graphene, to a good approximation, satisfies this condition, and the intensity of the $\bar{1}010$ diffraction spot should remain constant over a large range of tilt. Meyer *et al.*[33] have shown that this approach can be used to distinguish between single and bilayer graphene (in the case of bilayer graphene 4 orders of magnitude changes in diffracted spot intensity are expected). Figure 5e shows a diffraction pattern from GS supported by an amorphous carbon film. Figure 5f shows the changes in intensity for the $\bar{1}010$ diffraction spot as a function of tilt angle, confirming that the GS is indeed a single layer. The fact that the intensity of the $\bar{2}110$ diffracted spot is considerably lower than that of the $\bar{1}010$ spot provides additional confirmation of a single layer.[4]

The oxygen reduction and simultaneous transformation of the carbon sp^3 bonds into sp^2 can be explained by dehydration of XGO in DI water. If hydroxyl groups and hydrogen atoms are attached to two neighboring carbons, in an acidic environment they can combine through dehydration reaction, resulting in H_2O and GS with sp^2-bonded carbon atoms. For epoxy groups, the reduction is a two-step process. If an epoxy group is

attached to carbon atoms of GS with two hydrogen atoms attached to the neighboring carbons, in an acidic environment the system will first hydrate, transforming the epoxy group (−O−) to two hydroxyl groups (−OH), which then reduce to H_2O and GS with sp^2-bonded carbon atoms. Schematic diagrams for both reactions are presented in Figure 6. Since the presence of hydrogen atoms next to hydroxyl groups is needed for oxygen reduction, their availability will set the limit of oxygen reduction in the XGO to GS transformation, which can explain the presence of residual oxygen in the GS. Fourier transform infrared spectroscopy (FTIR) performed on XGO and GS specimens before and after transformation (Figure 7, for details see SI) supports dehydration as the main mechanism for oxygen reduction. Figure 7 shows significant reduction of the hydroxyl group[34] (2900−3600 cm^{-1}) and some reduction of epoxy groups.

To achieve deoxydation of XGO sheets in water, a low pH environment and moderately high temperature are needed. H^+ catalyst is essential for a dehydration reaction, where the kinetics of the reaction is governed by temperature (we observed a 4-fold reaction rate increase going from 95 to 120 °C). It should be noted that the deoxydation of XGO sheets can also take place in a basic environment with HO^- acting as a catalyst. Fan *et al.*[35] have reported deoxydation of graphene oxide sheets in alkaline water. In either case, the amount of hydrogen atoms bonded to carbon next to hydroxyl groups sets the limit of oxygen reduction. The role of H^+ catalyst in dehydration of XGO is the critical difference between oxygen removal processes in water and in air. Unlike reduction in water, extremely high temperatures (>600 °C) are needed to observe any considerable oxygen reduction in air due to direct thermal excitations.[11,16] In addition thermal reduction often generates CO_2, removing carbon from the sheets, resulting in defect formation and size reduction.

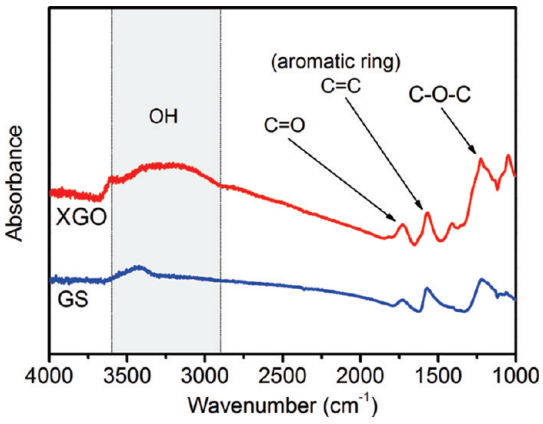

Figure 7. Fourier transform infrared spectra from XGO and GS. The spectra were recorded in transmission mode.

CONCLUSIONS

We successfully developed a hydrazine-free, high-yield method to produce single-layer graphene with high sp^2 fraction and conductivity at atmospheric pressure. Graphene sheets are reduced from exfoliated graphite oxide/graphene oxide in DI water at pH ≈ 3 within 48 h at a temperature of 95 °C. The graphene sheets produced according to this method have a resistivity comparable to graphene sheets produced using other methods. These measurements, combined with TEM observations, indicate that while these sheets are not fully reduced, the presence of large uniform interconnected oxygen-free patches with sp^2 carbon bonds is sufficient to provide sheets with electronic properties comparable to other reduced graphene sheets. We speculate that heating XGO for extended time in water provides enough energy for dehydration and transformation of C−C bonds from sp^3 to sp^2.

METHODS

Synthesis. A solution of 10 g of graphite (SP-1 graphite, from Bay Carbon) with average particle size of 30 μm, 200 mL of concentrated sulfuric acid (H_2SO_4 98%), and 5 g of sodium nitrate ($NaNO_3$) was prepared. Then 40 g of potassium permanganate ($KMnO_4$) was slowly added to the solution, while keeping the mixture in an ice bath to maintain a temperature of 35 °C. The solution was held in an ice bath until it reached 10 °C. The solution was then transferred into a bigger container and was diluted with 2 L of deionized water. Hydrogen peroxide (H_2O_2 30%) was then slowly added until the solution turned green. Graphite oxide was recovered from the solution after a four-step-wash procedure. After the reduction, the clear water was removed and the black precipitate was redispersed in 500 mL of dimethylformamide. The solution was then sonicated for 5 min and was slowly filtered through a PTFE membrane. The black film was dried in a vacuum oven (<0.05 bar) at 80 °C for 24 h. The dry film with metallic-like appearance was the GS film.

Characterization. A Digital Instrument Nanoscope III Multimode AFM at the College of Science and Engineering Characterization Facility of the University of Minnesota was used in noncontact mode for measurements. A Surface Science SSX-100 spectrometer was used to carry out XPS measurements. EA was conducted at Atlantic Microlab, Inc. For EA measurements the samples of XGO and GS were initially dried in a vacuum oven at 25 °C for 5 h.

Electrical Resistivity Measurements. Electrical resistance of XGO and GS films with different thicknesses was measured using the van der Pauw method. All samples were measured in a four-wire van der Pauw configuration with indium metal contacts. Measurements were made using an LR-700 ac resistance bridge at an excitation frequency of 20 Hz. All contacts were found to be ohmic down to the lowest temperature of measurement, and resistance anisotropies were small.

Transmission Electron Microscopy. For these experiments, FEI Tecnai F30 300 keV (S)TEM at the University of Minnesota was used. The microscope is equipped with a Schottky field emission gun and a high-resolution pole piece with a spherical aberration coefficient of C_s = 1.3 mm. The operational conditions of TEM were optimized to minimize possible electron-beam-induced damage. Under these conditions no visible specimen damage was observed during high-resolution TEM image acquisitions.

Acknowledgment. The authors would like to acknowledge Profs. A. Abdala, E. Aydil, A. Stein, and A. Bhan and Dr. H. Kim for helpful discussions and support from the Abu Dhabi-Minnesota Institute for Research Excellence (ADMIRE), a partnership between the Petroleum Institute of Abu Dhabi and the Department of Chemical Engineering and Materials Science of the University of Minnesota. This work was supported partially by the MRSEC Program of the NSF under Award Number DMR-0819885, as well as DMR-0804432. We also thank Mr. W. Xie and Drs. O. Ugurlu and G. Haugstad for technical support. This work utilized the University of Minnesota College of Science and Engineering Characterization Facility, which receives partial support from the NSF-NNIN program and capital equipment funding from the NSF through the MRSEC program.

Supporting Information Available: More information on synthesis, AFM, XPS, EA, TEM characterizations, and electrical resistivity measurements is provided. This material is available free of charge *via* the Internet at http://pubs.acs.org.

REFERENCES AND NOTES

1. Novoselov, K. S.; Geim, A. K.; Morozov, S. V.; Jiang, D.; Katsnelson, M. I.; Grigorieva, I. V.; Dubonos, S. V.; Firsov, A. A. Two-Dimensional Gas of Massless Dirac Fermions in Graphene. *Nature* **2005,** *438*, 197–200.
2. Zhang, Y. B.; Tan, Y. W.; Stormer, H. L.; Kim, P. Experimental Observation of the Quantum Hall Effect and Berry's Phase in Graphene. *Nature* **2005,** *438*, 201–204.
3. Novoselov, K. S.; Jiang, D.; Schedin, F.; Booth, T. J.; Khotkevich, V. V.; Morozov, S. V.; Geim, A. K. Two-Dimensional Atomic Crystals. *Proc. Natl. Acad. Sci. U. S. A.* **2005,** *102*, 10451–10453.
4. Hernandez, Y.; Nicolosi, V.; Lotya, M.; Blighe, F. M.; Sun, Z. Y.; De, S.; McGovern, I. T.; Holland, B.; Byrne, M.; Gun'ko, Y. K.; *et al* J. N. High-Yield Production of Graphene by Liquid-Phase Exfoliation of Graphite. *Nat. Nanotechnol.* **2008,** *3*, 563–568.
5. Tung, V. C.; Allen, M. J.; Yang, Y.; Kaner, R. B. High-Throughput Solution Processing of Large-Scale Graphene. *Nat. Nanotechnol.* **2008,** *4*, 25–29.
6. Berger, C.; Song, Z. M.; Li, X. B.; Wu, X. S.; Brown, N.; Naud, C.; Mayou, D.; Li, T. B.; Hass, J.; Marchenkov, A. N.;*et al*. Electronic Confinement and Coherence in Patterned Epitaxial Graphene. *Science* **2006,** *312*, 1191–1196.
7. Zhou, S. Y.; Gweo, G. H.; Fedorov, A. V.; First, P. N.; Heer, W. A. D.; Lee, D. H.; Guinea, F.; Neto, A. H. C.; Lanzara, A. Substrate-Induced Bandgap Opening in Epitaxial Graphene. *Nat. Mater.* **2007,** *6*, 770–775.
8. Kim, K. S.; Zhao, Y.; Jang, H.; Lee, S. Y.; Kim, J. M.; Ahn, J. H.; Kim, P.; Choi, J. Y.; Hong, B. H. Large-Scale Pattern Growth of Graphene Films for Stretchable Transparent Electrodes. *Nature* **2009,** *457*, 706–710.
9. Stankovich, S.; Dikin, D. A.; Piner, R. D.; Kohlhaas, K. A.; Kleinhammes, A.; Jia, Y.; Wu, Y.; Nguyen, S. T.; Ruoff, R. S. Synthesis of Graphene-Based Nanosheets *via* Chemical Reduction of Exfoliated Graphite Oxide. *Carbon* **2007,** *45*, 1558–1565.
10. Eda, G.; Fanchini, G.; Chhowalla, M. Large-Area Ultrathin Film of Reduced Graphene Oxide As a Transparent and Flexible Electronic Material. *Nat. Nanotechnol.* **2008,** *3*, 270–274.
11. Schniepp, H. C.; Li, J. L.; McAllister, M. J.; Sai, H.; Herrera-Alonso, M.; Adamson, D. H.; Prud'homme, R. K.; Car, R.; Saville, D. A.; Aksay, I. A. Functionalized Single Graphene Sheets Derived from Splitting Graphite Oxide. *J. Phys. Chem. B* **2006,** *110*, 8535–8539.
12. Kim, H.; Abdala, A.; Macosko, C. W. Graphene/Polymer Nanocomposites. *Macromolecules* **2010,** *43*, 6515–6530.
13. Lv, W.; Tang, D. -M.; He, Y.-B.; You, C.-H.; Shi, Z.-Q.; Chen, X.-C.; Chen, C.-M.; Hou, P.-X.; Liu, C.; Yang, Q.-H. Low-Temperature Exfoliated Graphenes: Vacuum-Promoted Exfoliation and Electrochemical Energy Storage. *ACS Nano* **2009,** *3*, 3730–3736.
14. Paci, J. T.; Belytschko, T.; Schatz, G. C. Computational Studies of the Structure, Behavior upon Heating, and Mechanical Properties of Graphite Oxide. *J. Phys. Chem. C* **2007,** *111*, 18099–18111.
15. Chattopadhyay, J.; Mukherjee, A.; Hamilton, C. E.; Kang, J.; Chakraborty, S.; Guo, W. H.; Kelly, K. F.; Barron, A. R.; Billups, W. E. Graphite Epoxide. *J. Am. Chem. Soc.* **2008,** *130*, 5414–5415.
16. Mattevi, C.; Eda, G.; Agnoli, S.; Miller, S.; Mkhoyan, K. A.; Celik, O.; Mostrogiovanni, D.; Granozzi, G.; Garfunkel, E.; Chhowalla, M. Evolution of Electrical, Chemical, and Structural Properties of Transparent and Conducting Chemically Derived Graphene Thin Films. *Adv. Funct. Mater.* **2009,** *19*, 2577–2583.
17. Stankovich, S.; Dikin, D. A.; Dommett, G. H. B.; Kohlhaas, K. M.; Zimney, E. J.; Stach, E. A.; Piner, R. D.; Nguyen, S. T.; Ruoff, R. S. Graphene-Based Composite Materials. *Nature* **2006,** *442*, 282–286.
18. Gilje, S.; Han, S.; Wang, M.; Wang, K. L.; Kaner, R. B. A Chemical Route to Graphene for Device Applications. *Nano Lett.* **2007,** *7*, 3394–3398.
19. Gomez-Navarro, C.; Weitz, R. T.; Bittner, A. M.; Scolari, M.; Mews, A.; Burghard, M.; Kern, K. Electronic Transport Properties of Individual Chemically Reduced Graphene Oxide Sheets. *Nano Lett.* **2007,** *7*, 3499–3503.
20. Zhou, Y.; Bao, Q.; Lena, A.; Tang, L.; Zhong, Y.; Loh, K. P. Hydrothermal Dehydration for the "Green" Reduction of Exfoliated Graphene Oxide to Graphene and Demonstration of Tunable Optical Limiting Properties. *Chem. Mater.* **2009,** *21*, 2950–2956.
21. Chen, C.; Yang, Q.-H.; Yang, Y.; Lv, W.; Wen, Y.; Hou, P.-X.; Wang, M.; Cheng, H.-M. Self-Assembled Free-Standing Graphite Oxide Membrane. *Adv. Mater.* **2009,** *21*, 3007–3011.
22. Chen, Y.; Zhang, X.; Zhang, D.; Yu, P.; Ma, Y. High Performance Supercapacitors Based on Reduced Graphene Oxide in Aqueous and Ionic Liquid Electrolytes. *Carbon* **2011,** *49*, 573–580.
23. Hummers, W. S., Jr.; Offeman, R. E. Preparation of Graphitic Oxide. *J. Am. Chem. Soc.* **1958,** *80*, 1339.
24. Szabo, T.; Berkesi, O.; Dekany, I. DRIFT Study of Deuterium-Exchanged Graphite Oxide. *Carbon* **2005,** *43*, 3186–3189.
25. Boukhvalov, D. W.; Katsnelson, M. I. Modeling of Graphite Oxide. *J. Am. Chem. Soc.* **2008,** *130*, 10697–10701.
26. Stankovich, S.; Piner, R. D.; Chen, X. Q.; Wu, N. Q.; Nguyen, S. T.; Ruoff, R. S. Stable Aqueous Dispersions of Graphitic Nanoplatelets *via* the Reduction of Exfoliated Graphite Oxide in the Presence of Poly(Sodium 4-Styrenesulfonate). *J. Mater. Chem.* **2006,** *16*, 155–158.
27. Mkhoyan, K. A.; Contryman, A. W.; Silcox, J.; Stewart, D. A.; Eda, G.; Mattevi, C.; Miller, S.; Chhowalla, M. Atomic and Electronic Structure of Graphene-Oxide. *Nano Lett.* **2009,** *9*, 1058–1063.
28. Hontoria-Lucas, C.; Peinando, A. J. L.; Lopez-Gonzalez, J. D. D.; Rojas-Cervantes, M. L.; Martin-Aranda, R. M. Study of Oxygen-Containing Groups in a Series of Graphite Oxides: Physical and Chemical Characterization. *Carbon* **1995,** *33*, 1585–1592.
29. Yang, D.-Q.; Sacher, E. Carbon 1s X-ray Photoemission Line Shape Analysis of Highly Oriented Pyrolytic Graphite: The Influence of Structural Damage on Peak Asymmetry. *Langmuir* **2006,** *22*, 860–862.
30. Eda, G.; Chhowalla, M. Chemically Derived Graphene Oxide: Towards Large-Area Thin-Film Electronics and Optoelectronics. *Adv. Mater.* **2010,** *22*, 2392–2415.
31. Du, X.; Skachko, I.; Barker, A.; Andrei, E. Y. Approaching Ballistic Transport in Suspended Graphene. *Nat. Nanotechnol.* **2008,** *3*, 491–495.
32. Li, X. L.; Zhang, G. Y.; Bai, X. D.; Sun, X. M.; Wang, X. R.; Wang, E.; Dai, H. J. Highly Conducting Graphene Sheets and Langmuir-Blodgett Films. *Nat. Nanotechnol.* **2008,** *3*, 538–542.
33. Meyer, J. C.; Geim, A. K.; Katsnelson, M. I.; Novoselov, K. S.; Booth, T. J.; Roth, S. The Structure of Suspended Graphene Sheets. *Nature* **2007,** *446*, 60–63.
34. Kosynkin, D. V.; Higginbotham, A. L.; Sinitskii, A.; Lomeda, J. R.; Dimiev, A.; Price, B. K.; Tour, J. M. Longitudinal Unzipping of Carbon Nanotubes to Form Graphene Nanoribbons. *Nature* **2009,** *458*, 872.
35. Fan, X.; Peng, W.; Li, Y.; Li, X.; Wang, S.; Zhang, G.; Zhang, F. Deoxygenation of Exfoliated Graphite Oxide under Alkaline Conditions: A Green Route to Graphene Preparation. *Adv. Mater.* **2008,** *20*, 4490–4493.